# Ionothermal Synthesis of Tailor-Made LiFePO4 Powders for Li-Ion Battery Applications

**ARTICLE** *in* CHEMISTRY OF MATERIALS · MARCH 2009

Impact Factor: 8.35 · DOI: 10.1021/cm803259x



**7 AUTHORS**, INCLUDING:

Nadir Recham
Université de Picardie Jules Verne
**38** PUBLICATIONS **1,109** CITATIONS
SEE PROFILE

Loic Dupont
Université de Picardie Jules Verne
**128** PUBLICATIONS **6,950** CITATIONS
SEE PROFILE

Dominique Larcher
Université de Picardie Jules Verne
**72** PUBLICATIONS **4,561** CITATIONS
SEE PROFILE

Michel Armand
Université de Picardie Jules Verne
**307** PUBLICATIONS **20,850** CITATIONS
SEE PROFILE

CHEMISTRY OF MATERIALS



Article

# Ionothermal Synthesis of Tailor-Made LiFePO Powders for Li-Ion Battery Applications

N. Recham, L. Dupont, M. Courty, K. Djellab, D. Larcher, M. Armand, and J.-M. Tarascon

*Chem. Mater.*, **2009**, 21 (6), 1096-1107• DOI: 10.1021/cm803259x • Publication Date (Web): 05 February 2009



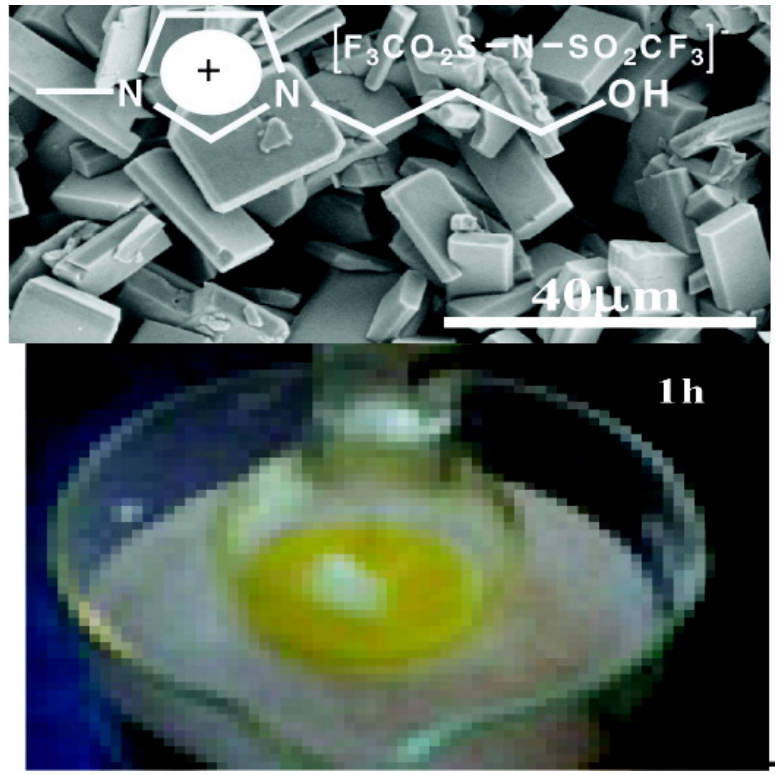


## More About This Article

Additional resources and features associated with this article are available within the HTML version:

- Supporting Information
- Access to high resolution figures
- Links to articles and content related to this article
- Copyright permission to reproduce figures and/or text from this article



Chemistry of Materials is published by the American Chemical Society. 1155 Sixteenth Street N.W., Washington, DC 20036

# Ionothermal Synthesis of Tailor-Made $LiFePO_4$ Powders for Li-Ion Battery Applications

N. Recham, L. Dupont, M. Courty, K. Djellab, D. Larcher, M. Armand, and J.-M. Tarascon*

*Laboratoire de Réactivité et Chimie des Solides, Université de Picardie Jules Verne, CNRS UMR6007, 33 rue Saint Leu, 80039 Amiens, France*

*Received December 3, 2008. Revised Manuscript Received January 12, 2009*

As opposed to ceramic methods, low-temperature solvothermal-hydrothermal methods using liquid media as reaction support are less energy demanding to design new electrode materials; therefore, they tend to replace ceramic routes. Here, we report the use of ionic liquids as both solvent and template to enable the growth of $LiFePO_4$ (LFP) powders with controlled size and morphology at temperatures at least 200 °C lower than those required for conventional ceramic methods, while showing excellent electrochemical performances versus lithium. An inherent advantage to the use of ionic liquids lies in the feasibility of carrying out the reaction at atmospheric pressure. Besides, the recovery of the powders from the reacting medium is particularly easy, as are the effluents and ionic liquid recycling. Additionally, it is shown that ionic liquids can be used as a structural directing agent to orient crystal growth and obtain powders adopting a single morphology. Needless to say, such a new approach, which is not specific to $LiFePO_4$, offers great opportunities for the low-temperature synthesis of new electrode materials.

## Introduction

Because of its attractive energy density and cycle-life performances, it has taken less than 20 years for the Li-ion technology to capture the portable electronic market. The question is: will such a technology be as quick to conquer the staggering upcoming markets of electric transportation (e.g., hybrid electric vehicles) and renewable energies? Although optimism must prevail, several hurdles remain to be cleared, with the top of the list being safety and cost.[1] Chemical advances in any of the cell components, whether they are anodes, electrolytes, or cathodes, can benefit the battery final cost and safety. Solid-state chemists[2] have played the leading role in addressing these issues by bringing to the scene $LiFePO_4$ (LFP) a material that, besides having the right voltage (3.5 V vs $Li^+/Li$) to present safety attributes, is a natural mineral known as triphyllite made of low cost and abundant elements. Mining and directly using $LiFePO_4$ is not an option, as both morphology and purity of this material have to be worked out to fight its intrinsically low conductivity and turn it into an attractive electrode material. Because of smart material processing enlisting both carbon coating[3] and particles downsizing processes,[4−6] $Li^+$ can presently be reversibly extracted out of $LiFePO_4$ leading to room temperature capacities of ∼160 mA h $g^{-1}$ (close to the theoretical value of 170 mA h $g^{-1}$).

Besides addressing fundamental aspects regarding the influence of particle size/defects or cationic/anionic substitutes on insertion/deinsertion mechanism and capacity/rate performances of $LiFePO_4$, a great amount of work is presently aimed at new low-cost processes to make highly electrochemically optimized $LiFePO_4$ powders.[1] Along that line, low-temperature hydro(solvo)thermal processes, which are energy miser compared with high-temperature ceramic routes, have received increased attention with successful results, among which the hydrothermal approach pursued by Whittingham's[7,8] or Tajimi's[9] groups, and more recently by Delacourt et al.[10] The latter shows the feasibility of precipitating at atmospheric pressure (e.g., via a solvothermal process) tailor-made $LiFePO_4$ nanopowders from a DMSO-based aqueous medium containing the suitable precursors ($H_3PO_4$, $FeSO_4$, and LiOH). Our group[11] also recently reported a new eco-efficient hydrothermal synthesis of $LiFePO_4$ with tunable morphologies, which relies on the use of "latent bases" capable of releasing a nitrogen-based base upon heating. Regardless of the specificity of the hydro(solvo)thermal approach, the carbon-coating of the resulting powders is always beneficial to their electrochemical performances.

* Corresponding author. E-mail: jean-marie.tarascon@sc.u-picardie.fr.

(1) Tarascon, J. M.; Armand, M. *Nature* **2001**, *414*, 359–367.
(2) Padhi, A. K.; Nanjundaswamy, K. S.; Goodenough, J. B. *J. Electrochem. Soc.* **1997**, *144*, 1188–1194.
(3) Ravet, N. et al. *196th Meeting of the Electrochemical Society*; Honolulu, HI, Oct 17−22, 1999; Electrochemical Society: Pennington, NJ, 1999; abstract # 127.
(4) Delacourt, C.; Poizot, P.; Levasseur, S.; Masquelier, C. *Electrochem. Solid- State Lett.* **2006**, *9*, A352−A355.
(5) Nuspl, G., Wimmer, L., and Eisgruber, M. World Patent WO 2005/051840 A1, 2005.
(6) Meetong, N.; Huang, H.; Speakman, S.; Carter, W. C.; Chiang, Y. M. *Adv. Funct. Mater.* **2007**, *17*, 1115–1123.
(7) Chen, J.; Wang, S.; Whittingham, M. S. *J. Power Sources* **2007**, *174*, 442–448.
(8) Chen, J.; Vacchio, M. J.; Wand, S.; Chernova, N.; Zavalij, P. Y.; Whittingham, M. S. *Solid State Ionics* **2008**, *178*, 1676–1693.
(9) Jin, B-; Gu, H.-B. *Solid State Ionics* **2008**, *178*, 1907–1914.
(10) Delacourt, C.; Poizot, P.; Masquelier, C. World Patent, WO 2007/0051, 2007.
(11) Recham, N.; Laffont, L.; Armand, M.; Tarascon, J. M. *Electrochem. Solid-State Lett.* **2009**, *12* (2), A39−A44.

10.1021/cm803259x CCC: $40.75 
Published on Web 02/05/2009

Searching for alternative low-temperature syntheses, the ionothermal synthetic approach, which is based on the use of ionic liquids instead of water as solvent, appears quite attractive.[12] Like water, ionic liquids resulting from compatible cationic/anionic pairs have excellent solvent properties, but in addition they possess high thermal stability and negligible volatility so that the use of autoclave is not mandatory. Moreover, because of the flexible nature of the cationic/anionic pairs, they present, as solvents, great opportunities to purposely direct nucleation. Over the past decade, ionothermal synthesis has developed into an advantageous synthetic technique for the preparation of zeotypes[13] and other porous materials such as metal organic framework compounds (MOFs),[12] but there has been very limited use made of this technique in the synthesis of inorganic compounds. This is somewhat surprising, as it is claimed that ionothermal methods could in principle be used in any situation where hydrothermal or solvothermal methods have been successfully implemented.

In light of the aforementioned reports, we decided to explore the ionothermal synthesis of electrode materials, and we succeeded in preparing electrochemically active $LiFePO_4$ powders as reported herein. The paper will mainly focus on assessing the effect of various ionic liquid architectures on the morphology and electrochemical performances of $LiFePO_4$ powders, and will address the possibility of easily recovering the ionic liquids because of their purposely selected hydrophobic nature.

## Experimental Section

The X-ray powder diffraction patterns were recorded either on a Bruker D8 Diffractometer using a Co Kα radiation ($\lambda_1 = 1.78919$ Å, $\lambda_2 = 1.79321$ Å), equipped with a Gobel mirror, a Braun PSD (position sensitive detector) detector and operating at 40 kV and 30 mA in the range $2\theta = 10-45°$ with a $2\theta$ step size of 0.017° or on Bruker D8 Advance diffractometer (Cu Kα radiation, $\theta-2\theta$ geometry, linear Vantec counter). Lattice parameters were obtained from full pattern matching refinements via the Fullprof program (Windows version, March 2007)[14] using the pseudo-Voigt profile function of Thompson, Cox, and Hastings.[15] The morphology of the samples was studied by field-emission gun scanning electron microscopy (FEI Quanta 200 F). For the sake of electrical conduction, the powders were covered with a very thin layer of gold by metal pulverization. The high-resolution transmission electron microscopy images were taken with a Tecnai S-Twin F20.

DSC experiments were carried out on a Netzsch DSC 204F1 heat flux differential calorimeter at a heating rate of 2 °C $min^{-1}$ under a constant argon flow of 200 mL/min. The calibration was performed with gallium, $KNO_3$, indium, tin and bismuth references. Afterward, the samples were placed in aluminum pans covered with a pierced lid. Unless specified, the samples were heated from 30 °C up to 250 °C and held at this temperature for 24 h. Prior to each experiment a blank curve was recorded using an empty aluminum sample pan as a reference. The reported curves are corrected by subtracting the blank curve. Because we are here working under constant pressure conditions, the integration of the heat flow (W/g) signal as a function of time gives us access to the values of the variations in enthalpy of the reaction (ΔH°, J/g, J/mol). The values are reported per mole of precursor ($LiH_2PO_4$, $FeC_2O_4 \cdot 2H_2O$) and per mole of $LiFePO_4$ product.

Electrochemical characterization was performed using Swagelok-type cells. Positive electrodes were prepared by shock-milling (Speck 800) a powder mixture containing 85 wt % active material with 15 wt % SP (MM, Belgium) carbon, as electronic conductor. The cells were assembled in an argon-filled glovebox with 10 mg of the carbon/material mix separated from the negative electrode (lithium foil) by 2 sheets of glass fiber disks, the whole set-up being soaked in a $LiPF_6$ (1M) solution of ethylene carbonate (EC)/dimethyl carbonate (DMC) mixture (1/1 w/w). An aluminum current collector was used as the positive side to avoid electrolyte decomposition at high potential. Unless otherwise specified, galvanostatic tests were conducted with a MacPile (Claix, France) controller at a constant temperature of 25 °C.

## Results

Whatever the low-temperature solvothermal/hydrothermal synthesis reactions are, they basically consist in reacting in liquid media the corresponding metal/non metal-based soluble salt precursors, and increasing the temperature to promote the precipitation and growth of the desired phase. The present approach falls within the same synthesis strategy, with the only difference that the liquid media will rely on ionic liquids rather than water, which has good solvating properties too.

Ionic liquids are salts that differ from inorganic salts such as NaCl ($T_f = 801$ °C) because their melting temperature is lower than 100 °C. They are made of organic cations and anions, the choice/combination of which will affect not only their fusion temperature but also their solvating properties. Although they have been slow in entering the field of inorganic chemistry as alternative solvents for synthesis, their use has been flourishing in the field of organics, chemistry, electrochemistry, and catalysts. So there exists a colossal amount of groundwork[16,17] on how the effect of cations nature (pyridinium vs imidazolium), cations substitutions (alkyl-chains vs OH or CN termination), and changes in the nature of the anion (from fluorinated ($TFSI^-$) to nonfluorinated ($Cl^-$)), rule their physical/chemical properties; namely, their hydrophobicity, melting point, viscosity, solubility, and more relevant to this paper, their polarity that governs their solvating capability. It is, for instance, well-established that the length of cations alkyl chain affects their polarity, with the highest polarities being obtained for the shortest chains or chains having inserted nitrile, alcohol, or ketone groups. Hundreds of ionic liquids have been reported, but we initially focused on those with known thermal stability. More specifically, we selected (EMI-TFSI) 1-ethyl-3-methylimadozolium bis (trifluoromethanesulfonyl imide) (Solvionic, 115 ppm water content) as reacting medium to conduct our

(12) Parnham, E. R.; Morris, R. E. *Acc. Chem. Res.* **2007**, *40*, 1005–1013.
(13) Lin, Z.-J.; Li, Y.; Slawin, A. M. Z.; Morris, R. E. *Dalton Trans.* **2008**, 3989–3994.
(14) Rodríguez-Carvajal, J. Recent Developments of the Program FULLPROF. In *CPD Newslett.* **2001**, *26*, 12; available at http://www.iucr.org/iucr-top/news/index.html. The program and documentation can be obtained from http://www.ill.fr/dif/Soft/fp.
(15) Thompson, P.; Cox, D. E.; Hastings, J. B. *J. Appl. Crystallogr.* **1987**, *20*, 79–83.
(16) Papaiconomou, Ni.; Yakelis, N.; Salminen, J.; Bergman, R.; Prausnitz, J. M. *Thesis Report*; Lawrence Berkeley National Laboratory: Berkeley, CA, 2005.
(17) Ueki, T.; Watanabe, M. *J. Am. Chem. Soc.* **2008**, *41*, 11.

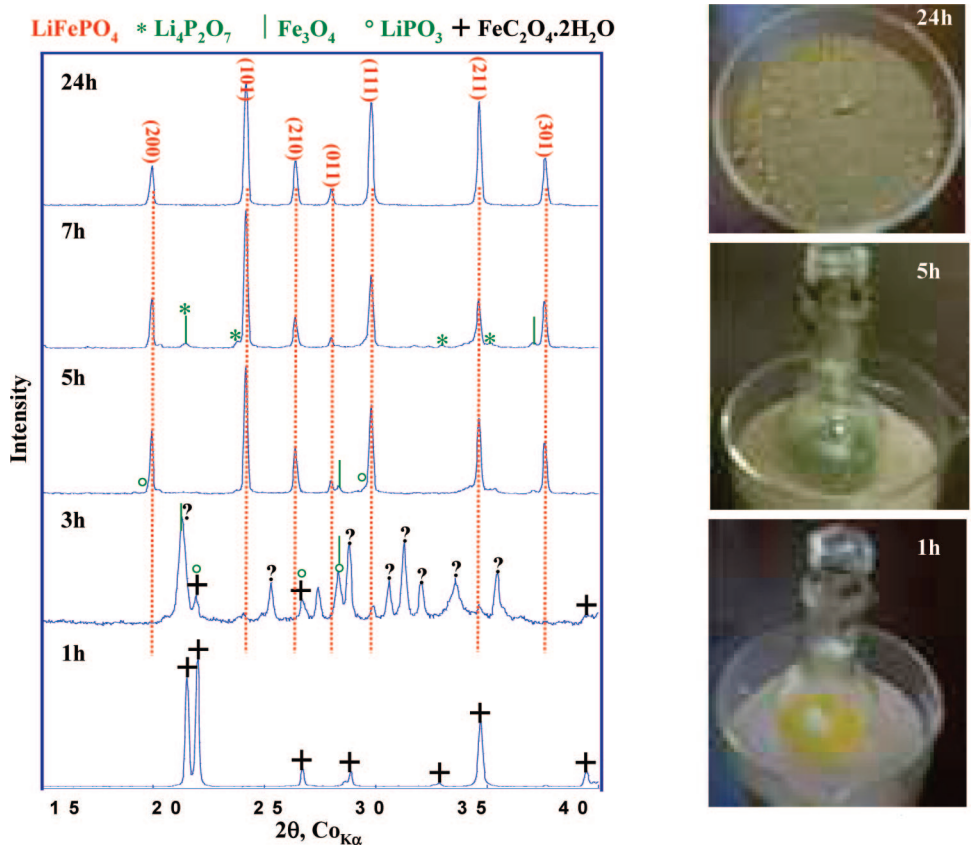


**Figure 1.** Synthesis of $LiFePO_4$ via the use of glass flask container. Left: the structural evolution of reactive mixture, containing stoichiometric amounts of $LiH_2PO_4$ and $FeC_2O_4 \cdot 2H_2O$ in 15 mL of (1-ethyl-3-methylimidazolium Bis(TriFluoromethaneSulfonyl)Imide) (= EMI-TFSI) ionic liquid, is monitored by X-rays as a function of time. To do so, eight flasks containing identical mixtures were prepared and heated up to 250 °C for various amounts of time, and the XRD patterns were collected (see text). Right, the color evolution of the suspensions when the reaction is conducted in a round flask.

first experiments and Fe oxalate ($FeC_2O_4 \cdot 2H_2O$) and $LiH_2PO_4$ as Fe- and Li-based precursors because of their anticipated slight solubility in EMI-TFSI, respectively.

Typical experiments were conducted in 50 mL glass flasks (Figure 1, right) according to the following protocol. Stoichiometric amounts of $FeC_2O_4 \cdot 2H_2O$ (99%, Aldrich) and $LiH_2PO_4$ (99%, Aldrich) powders to prepare 0.8 g of $LiFePO_4$ together with 5 mL of EMI-TFSI were placed in a 50 mL flask. After 10 min of stirring, the flask containing the suspension was placed in an oven, and its temperature was increased up to 250 °C at a rate of 5 °C/min. The suspension was maintained at that temperature for 24 h and then left to cool to ambient temperature. At the end of synthesis, powder and ionic liquid were separated by centrifugation. The recovered greenish powder was washed with 50 mL acetone, twice with 50 mL of distilled water, and finally with 50 mL of acetone and then oven-dried at 60 °C. The resulting powder had an Fe/P ratio of one (±0.02) as deduced from EDS analysis, and its XRD pattern (Figure 1 top left) indicates the presence of the single-phase $LiFePO_4$, as all the peaks were entirely indexed in the space group *Pnma* with $a = 10.331(3)$ Å, $b = 6.007(1)$ Å, $c = 4.691(1)$ Å, and $V = 291.1(1)$ Å$^3$, in good agreement with literature reports.[2,4,7] If not otherwise specified, such an ionothermal process was found to give a yield of about 99%, which simply implies a full yield considering the eventual losses during the recovery of the powder.

After each experiment, the ionic liquid is recovered and regenerated according to the following process so that it can be used again. The process consists in first twice washing the reaction supernatant with concentrated HCl solutions in order to get rid of traces of powder or solid impurity that could remain after centrifugation. Afterward, the supernatant is twice washed with water to eliminate HCl traces, and then diluted with dichloromethane ($CH_2Cl_2$) to separate it from water. Finally, dichloromethane is stripped with rotary evaporator, leaving behind the regenerated ionic liquid having a water content of 200 ppm, as deduced by Karl Fischer measurements. The yield of such washing process approaches 90%, and can easily be increased to the expense of further solvent handling by washing the recouped product with acetone or $CH_2Cl_2$, and by mixing the same liquid with the supernatant ionic liquid resulting from the centrifugation. So after being washed and dried, the ionic liquid can be used again for a new synthesis, which is a plus from an economical point of view. Such a recovery process better applies to hydrophobic ionic liquids and also some water miscible ILs when the partition coefficient is in favor of polar hydrophobic solvents like $CH_2Cl_2$ or CHFs (partially fluorinated hydrocarbons), which are easy to distill.

At this juncture, it should be stressed that regardless of the reacting time, synthesis temperatures lower than 200 °C never lead to the production of $LiFePO_4$. This comes as a surprise since we know that $LiFePO_4$ can be made at temperatures as low as 120 °C via solvothermal reaction in aqueous media.[4] Poorer solubility of the precursors in EMI-TFSI rather than in water was suspected of being responsible for such an observation. In contrast to $LiH_2PO_4$, which is

fully soluble in water, the solubility of $FeC_2O_4 \cdot 2H_2O$ is limited and reported to equal 2.2 and 2.6 g/L at 25 and 100 °C, respectively. To make further progress, as no such data exist with ionic liquids, we determined the solubility of our precursors in EMI-TFSI as follows. Two grams of $LiH_2PO_4$ were placed into 10 mL of EMI-TFSI, and the suspension was heated to various temperatures (up to 200 °C in steps of 40 °C with 1 h of resting time at each temperature) under constant stirring. For each temperature set, after stopping the stirring for 10 min, 1 mL aliquots were withdrawn and added to 3 mL of water so as to solubilize the remaining $LiH_2PO_4$ precursor. The water fraction was separated from the ionic liquid one (e.g., via phase separation), recovered, and evaporated via the use of a Rotavapor, and the residue (e.g., $LiH_2PO_4$) was weighed. Blank experiments consisting in putting 3 mL of water in 1 mL of EMI-TFSI were conducted in parallel; this was done in order to eliminate errors coming from the slight solubility of EMI-TFSI in water that could distort our measurements. From the weight of both recovered and initial precursors per milliliter of solution, we deduced the solubility of $LiH_2PO_4$ in EMI-TFSI to be 5.4 and 11.9 g/L at 80 and 200 °C, respectively. To measure $FeC_2O_4 \cdot 2H_2O$ solubility, 2 g of precursor was introduced in 10 mL of EMI-TFSI. Two milliliters of aliquots were withdrawn as before at various temperatures, and the oxalate was separated from the ionic liquid by centrifugation, washed with acetone, and weighed. Within the accuracy of the measurement, we detected no solubility for $FeC_2O_4 \cdot 2H_2O$, hence questioning the ionic liquid function during ionothermal synthesis.

To grasp further insight into the reacting path leading to the formation of $LiFePO_4$, we monitored, in a semi *in situ* way, the nature of the phases formed as a function of the annealing temperature and reacting time at a set temperature. For reasons of conciseness the data will solely be reported for one temperature; $T = 250$ °C. To do so, eight independent 50 mL glass flasks were filled with 5 mL of EMI-TFSI and 2.5 mmol of the precursors (0.2624 g $LiH_2PO_4$ and 0.4543 g $FeC_2O_4 \cdot 2H_2O$), and stirred at ambient temperatures for 20 min. Afterward, all of the flasks were placed into a sand bed, which temperature was raised to 250 °C in 2 h, and separately removed after periods of 1, 2, 3, 4, 5, 6, 7, and 12 h, respectively. Once cooled to room temperature, the powders were recovered as described prior to being dried and characterized by XRD. Figure 1 (left) shows the evolution of the collected patterns with, for $t = 1$ h, the sole presence of $FeC_2O_4 \cdot 2H_2O$ phase, and for $t = 3$ h, the presence of a multiphased sample. Besides the tiny remaining amount of oxalate, we could note the first hints of evidence for the growth of the $LiFePO_4$ phase as indicated by the red dashed lines together with extra peaks (denoted by ? in Figure 1) that we could not unambiguously assign even though some of them could indicate the presence of $Fe_3O_4$ and $LiPO_3$. $LiH_2PO_4$ appears in neither of the reported XRD patterns, as it is soluble in water and removed during the washing step. Longer reaction times result in the growth of $LiFePO_4$ so that the material becomes single-phased after 24 h. In contrast, we never succeeded in producing $LiFePO_4$ at 220 °C, regardless of the reacting time we tried.

To assess the thermal stability of both the precursors and their reacting mixtures, since they could simplify our understanding of the ionothermal growth mechanism of $LiFePO_4$, we performed DSC measurements using similar heating conditions as above (e.g., heating rate of 2°/min, temperature, and time). To decipher the role of the ionic liquid, two sets of experiments were conducted; they consisted in heating the precursors and mixture of precursors in the absence (top curves in panels a, b, and c in Figure 2) or the presence of the ionic liquid EMI-TFSI (bottom curves in panels a, b, and c in Figure 2). From Figure 2 (top and middle panels), it is clear that the decomposition/dehydration process for $LiH_2PO_4$ or $FeC_2O_4 \cdot 2H_2O$ is not modified by the presence of the ionic liquid since the shape, position and related variation in enthalpies for the endothermic signals are very close. Only the decomposition temperature of the oxalate is slightly altered. This is further demonstrated by the XRD patterns showing the formation of $FeC_2O_4$ at 250 °C, whether EMI-TFSI is present or not. For $LiH_2PO_4$, XRD patterns are not shown because the dehydrated phosphate, in both cases, quickly uptakes water as soon as exposed to air, leading to a non-crystalline solid. From these data, it is clear that the ionic liquid is not significantly modifying the decomposition temperature or the decomposition reaction products of the precursors. In contrast, it is very interesting to note that the thermal behavior of a mixture of the precursors very much depends on the presence of the ionic liquid (Figure 2, bottom panel). The DSC trace for a stoichiometric mixture of $LiH_2PO_4$ and $FeC_2O_4 \cdot 2H_2O$ is roughly the sum of the individual traces, in terms of signal intensity, shape and position (aside from again a slight modification of the oxalate decomposition temperature), indicating that both precursors are independently decomposing and not reacting in this temperature range as confirmed by the XRD pattern collected on the heated samples. In the presence of EMI-TFSI, the shape of the DSC signal and the nature of the products of decomposition are totally different, with mainly the presence of crystallized $Li_4P_2O_7$ as opposed to crystallized dehydrated $FeC_2O_4$ and amorphous phosphate (as indirectly deduced by HRTEM) for the ionic-liquid-free mixture. This clearly indicates that the ionic liquid plays a key role in the decomposition reaction of the mixture. It most likely triggers an alternative reaction path, which proceeds via the solution, hence lowering the temperature of preparation of $LiFePO_4$, as we are now dealing with soluble and reactive species rather than with a slow solid-state species migration as in the ceramic process. In light of these DSC results, our inability to prepare $LiFePO_4$ powders at 220 °C, even after 48 h of reaction, while they can be prepared in 12 or 24 h at 250 °C, most likely lies in kinetic issues as at 220 °C the precursor's reactivity is not sufficient yet.

To further support the above solution vs ceramic comparison, $FeC_2O_4 \cdot 2H_2O$ and $LiH_2PO_4$ powders were thoroughly mixed, pressed into pellets, and annealed under argon atmosphere. Regardless of the reaction time, no sign of $LiFePO_4$ formation could be detected at 250 °C. To see signs of $LiFePO_4$ formation, temperatures as high as 450 °C were needed, indicating the benefits of ionic liquids in lowering the synthesis temperature by at least 200 °C as compared to

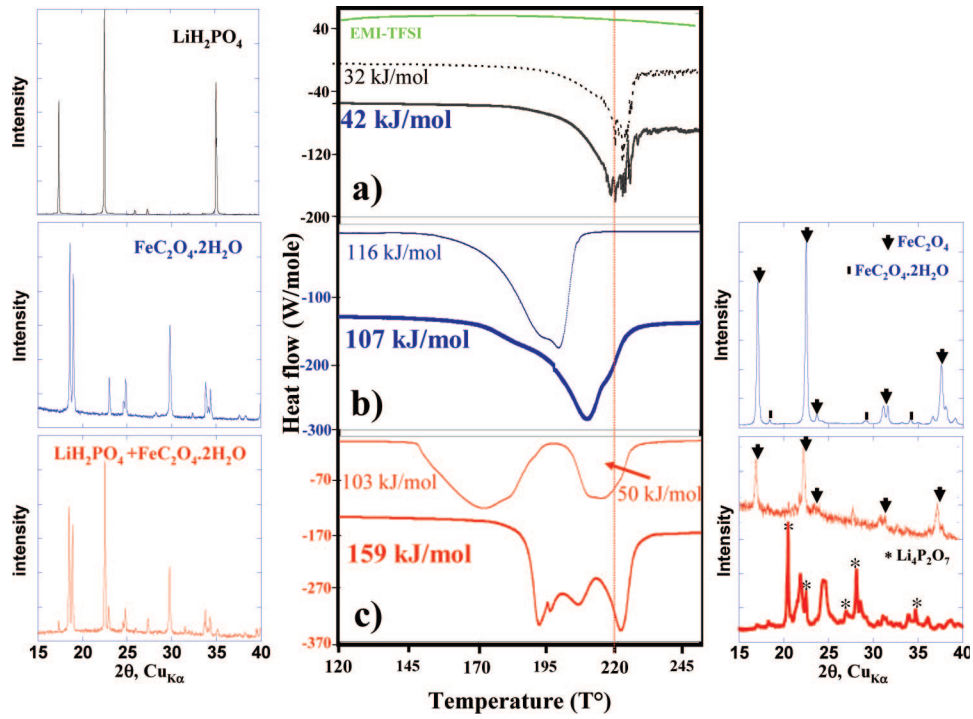


**Figure 2.** DSC traces collected in open Al pans, under argon flow and at a 2°/min rate (center row), together with XRD patterns of the initial materials (left row) and recovered samples after being cooled down and exposed to air (right row). A blank run performed with EMI-TFSI alone is shown at the top of (a) together with the signals recorded for $LiH_2PO_4$ with and without EMI-TFSI, (b) $FeC_2O_4 \cdot 2H_2O$ with and without EMI-TFSI, (c) 1/1 molar mixture of $LiH_2PO_4$ and $FeC_2O_4 \cdot 2H_2O$, with and without EMI-TFSI. In each DSC panel, the top trace is for powders without ionic liquid, the bottom is for a suspension in ionic liquid. The 24 h heating step at 250 °C, which corresponds to the growth of the $LiFePO_4$ phase, is not reported as the curve was featureless. Values for the variations in enthalpies are reported per mole of precursor (e.g., $LiH_2PO_4$, $FeC_2O_4 \cdot 2H_2O$). On the left, we have reported the XRD patterns of the precursor phases or mixtures, and on the right, the XRD patterns of the reacting products once they had been through the DSC cycle. The XRD patterns (bottom right) bear the most meaningful differences to distinguish the role of the ionic liquid.

classical ceramic approaches. Even greater differences were obtained, as we experienced the feasibility of growing $LiFePO_4$ at 180 °C in EMI-TFSI but using more soluble precursors such as $FeCl_2$, for instance.

This new insight regarding the nucleation/growth of $LiFePO_4$ led us to consider how varying the precursor/ionic liquid ratio could affect the $LiFePO_4$ particle size. The reason is that any direct nucleation/growth process taking place in solution is known to strongly depend on the precursor's concentration and temperature.[18] Increasing concentration or temperature or both should lead to smaller particles, because of the greater number of seeds forming and their smaller critical radius.[19] In addition, when particles are getting small, the need to minimize their surface energy can go through a preferential dissolution for the benefit of larger ones (Ostwald ripening),[20] and occasionally the coexistence of these two superimposed reverse processes can result in a minimum in stable particles size. In light of such considerations we have conducted various syntheses by varying the $LiH_2PO_4$ and $FeC_2O_4 \cdot 2H_2O$ precursor concentration from $1 \times 10^{-3}$, $2.5 \times 10^{-3}$, and $1 \times 10^{-2}$ mol/L in EMI-TFSI, although we were well aware that we are dealing more with suspensions rather than pure solutions in our system. Nevertheless, we noted (Figure 3) that the particle size goes through a minimum for the intermediate concentration, providing then further evidence for a solution-driven mechanism. Last, it is worth mentioning in the present context that we observed experimentally a coarsening of the particle with increasing the reacting time from 24 to 48 h.

Although the above experiments fall short of elucidating details of the reacting path leading to the ionothermal growth of $LiFePO_4$, they have the merit of stressing that its growth temperature is a function of the ability of the ionic liquid to trigger the decomposition temperature of the precursor while highlighting the importance of having precursor solubility. Such a finding leads us to either use other well-known ionic liquids or design new ones. This was done by playing either on the cation−anion combination or on the cation itself, via its functionalization by alkyl chains. For the latter, the length of the carbon alkyl chain was first increased; a CN (nitrile) group or an OH (alcohol) group was then introduced at the end of the carbonic chain to modulate its lipophilic/polar character. Although the reactions can be done in glass flasks, for handling reasons linked to the need to operate at 250 °C, we used a 50 mL PTFE Teflon-lined autoclave (Parr Instruments). The experimental protocol, previously described to prepare $LiFePO_4$ in a glass flask, was literally duplicated with the only difference that the autoclaves were placed in an oven rather than in a sand bed during the heating step process.

Out of the various ionic liquids we have tried (Figure 4), we found only three (Table 1) that could not permit the formation of $LiFePO_4$ at 250 °C or even higher temperature (until the decomposition temperature of the ionic liquid).

(18) LaMer, V. K.; Dinegar, R.H, *J. Am. Chem. Soc.* **1950**, *72* (11), 4847–4854.
(19) Köhler, H. N. *Trans. Faraday Soc.* **1936**, *32*, 1152.
(20) Ostwald, W. Z. *Z. Phys. Chem.* **1901**, *37*, 385.

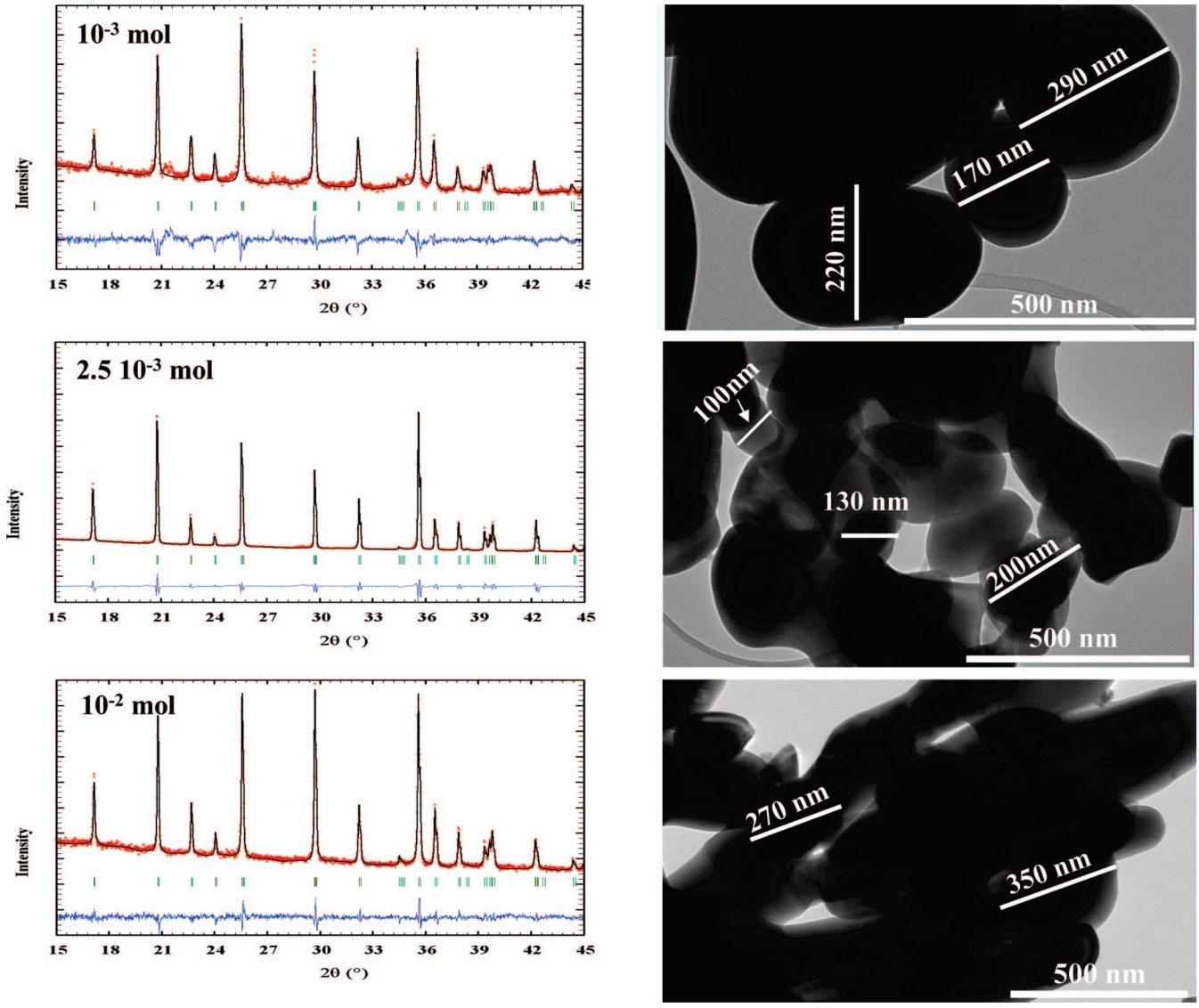


**Figure 3.** Effect of precursor concentration on the structure (XRD) and morphology (SEM) of the $LiFePO_4$ powders. The experiments were carried out at 250 °C in glassware containers using EMI-TFSI as ionic liquid and $LiH_2PO_4$, $FeC_2O_4 \cdot 2H_2O$ precursors having concentrations ranging from $1 \times 10^{-3}$, $2.5 \times 10^{-3}$, and $1 \times 10^{-2}$ mol/L.

Among them is 1-butyl-1-methylpyrrolidium bis(trifluoromethanesulfonyl)imide, containing a pyrrolidinium rather than an azolium cation. This raises the question of the possible role of the C2- acidic proton in the imidazolium cation. Yet, 1,2-dimethyl-3-propyl imidazolium without C2 proton enabled the formation of the phosphate phase. So another explanation remains to be found. Besides, we note that maintaining the 1-butyl-3-methylimidazolium or 1-ethyl-3-methylimidazolium cations but changing the bis(trifluoromethanesulfonyl)imide anion by either a tetrafluoroborate ($BF_4^-$) or a tricyanomethide ($C_4N_3^-$) anion also prevents the formation of $LiFePO_4$. DSC measurements aiming to check the reactivity of these various ionic liquids with both $LiH_2PO_4$ and $FeC_2O_4 \cdot 2H_2O$ are presently being conducted with the hope of providing a rational explanation for their nonsuitability as liquid media to prepare $LiFePO_4$ powders.

Besides, through this survey, we also found that the nature of the used ionic liquid does slightly change $LiFePO_4$ growth temperature, which can be lowered from 250 to 200 °C with OH-based ionic liquid. In contrast, it drastically affects the morphology and particle size of the obtained $LiFePO_4$ powders together with their XRD signatures as clearly shown in Figure 5 with namely the growth of some reflections at the expense of others, which indicates a preferential orientation growth. Spectacularly, by plotting the (101)/(200) $LiFePO_4$ XRD intensity ratio as a function of the used ionic liquid media (Figure 5), we note that the presence of the CN group drastically favors the intensity of the (101) Bragg peak while long alkyl chains (C18) favor the (200) one.

At this juncture, to both understand the formation mechanism of $LiFePO_4$ particles in the liquid ionic and determine the shape of the particles implying the preferential orientation observed on the XRD pattern, an in situ TEM study was undertaken. The particles grown in the CN-based ionic liquid are considered first.

Thanks to topochemistry, all of the steps of the reaction could be observed on the same sample. Figure 6 shows the evolution of the shape and size of the different particles of $LiFePO_4$ versus reaction time. In the early stage, very small

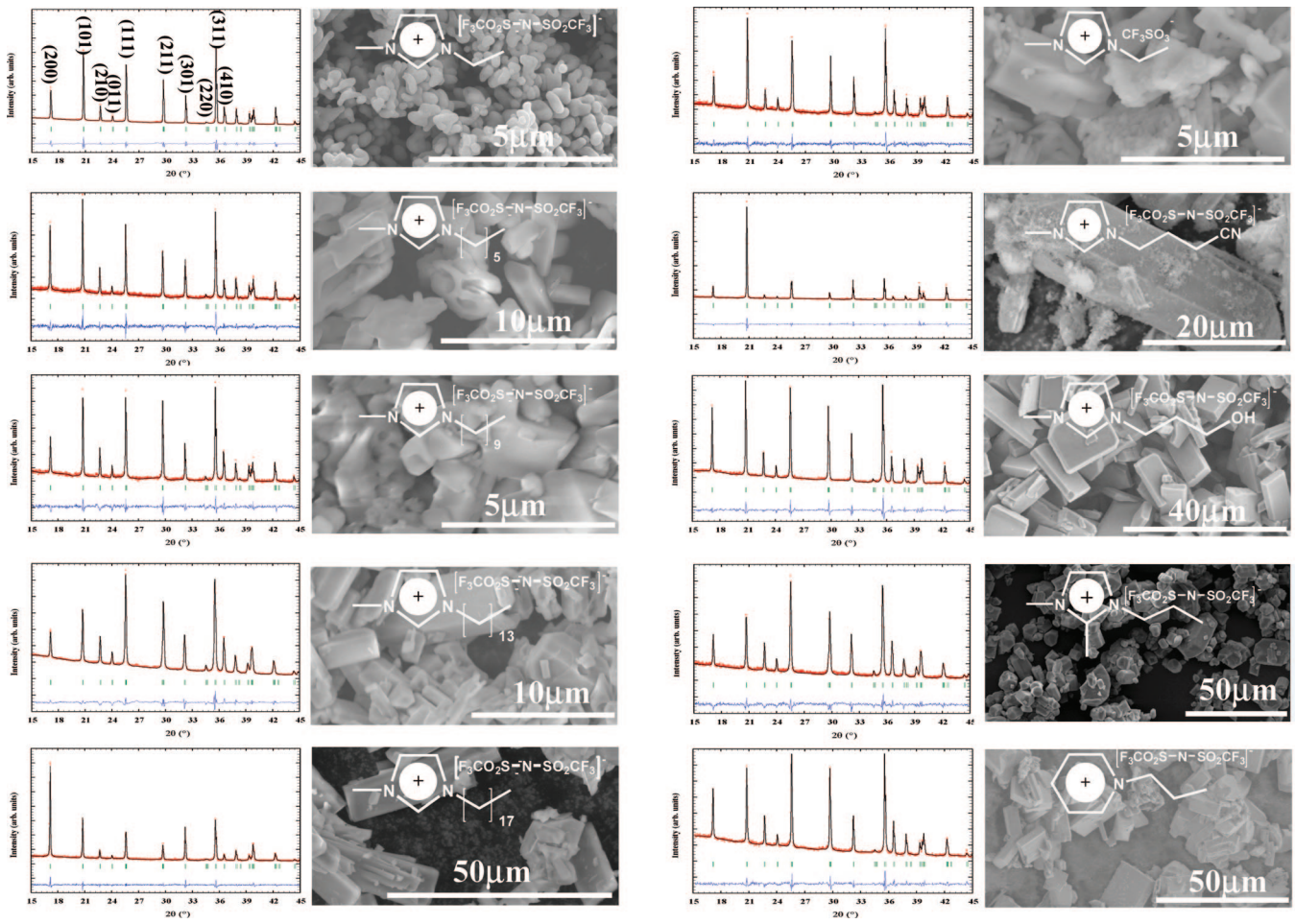


**Figure 4.** XRD patterns and SEM photographs for various $LiFePO_4$ samples obtained via the use of various ionic liquids while maintaining identical concentrations of the $LiH_2PO_4$ and $FeC_2O_4 \cdot 2H_2O$ precursors. Regardless of the ionic liquid used, the reactions were conducted in autoclaves using ramping temperatures of 2 °C/min until 250 °C and maintaining the samples at these temperatures for 24 h.

LFP particles (less than 100 nm) are formed (Figure 6a). Then, these primary particles gather together in order to form thin needles (Figure 6b). The size of these needles is about 1 $\mu$m long by less than 100 nm wide. The most remarkable point is that, during the maturing step, all of these needles pile up in such a perfect way that a very long needle grows (Figure 6c). It is worth noting that the long axis of the initial small needles becomes the width of the final large needle. At the end, a thick and long needle of several tens of micrometers long by 1 or 2 $\mu$m wide is obtained (Figure 6d). A needle shape could explain the preferential orientation observed by XRD, but in light of the growth mechanism, it is amazing that small individual needles perfectly pile up to form a single crystal. Figure 7 clearly shows the densification process leading to the single crystal needle. Through the observation of images taken at different magnifications on the same particle (Figure 7a−c), a Lego-type building process is suggested. Indeed, each small needle could be compared to a Lego brick that could be added to the existing stacking in only one way (inset in Figure 7b). Consequently, each brick shows the same orientation as observed on the high-resolution image (Figure 7c), and according to the punctual SAED (selected area electron diffraction) pattern (Figure 7d), the particles lie on the (101) plane consistent with the preferential orientation observed by XRD. Such a TEM study reveals the type of reaction leading to large oriented single crystals of LFP. After dissolution of the reactants, thin needles precipitate out of the solution then a solid−solid coarsening reaction occurs, and a large needle grows from the small ones (white arrow, Figure 7c). So in this case, it looks like the ionic liquid plays the role of both solvent and surface growth directing template agent.

To make further progress and determine the reason why the [200] growth orientation is not privileged for $LiFePO_4$ particles grown in C18-based EMI-TFSI ionic liquid, a TEM study was also realized on these particles. The particles are quite different from the previous sample: they are denser and the ratio between the length and the width is much smaller: 6 $\mu$m by 4 $\mu$m particles could easily be obtained (Figure 8a). According to collected SAED patterns (Figure 8b), they are all lying on the same (200) plane, which is consistent with the preferential orientation observed on XRD diagrams. In terms of nucleation and growth process, the mechanism is much more straightforward. Indeed, the HRTEM images recorded on the edge of the particles reveal no brick or domains but well-crystallized and dense crystallites (Figure 8c)

To check the electrochemical performances on the various batches of $LiFePO_4$ powders, Swagelok-type half-cells were assembled in an argon-filled glovebox. The cells, if not otherwise specified, were cycled at a rate of one lithium in

**Table 1. Formulae of the Various Ionic Liquids That We Have Used Are Listed Together with the Temperatures at Which They Could Enable the Formation of $LiFePO_4$ Powders**

| Formula | Name | $LiFePO_4$ obtained | Reaction T (°C) |
|---|---|---|---|
| 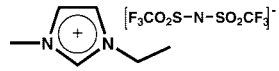 | 1-ethyl-3-methylimidazolium Bis(trifluoromethanesulfonyl)imide (EMI-TFSI) | Yes | 250 |
| 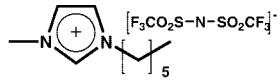 | 1-ethyl-3-hexylimidazolium Bis(trifluoromethanesulfonyl)imide (C6) | Yes | 250 |
| 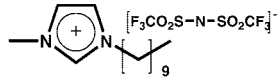 | 1-decyl-3-methylimidazolium Bis(trifluoromethanesulfonyl)imide (C10) | Yes | 250 |
| 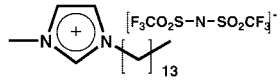 | 1-tetradecyl-3-methylimidazolium Bis(trifluoromethanesulfonyl)imide (C14) | Yes | 250 |
| 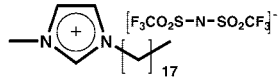 | 1-octadecyl-3-methylimidazolium Bis(trifluoromethanesulfonyl)imide (C18) | Yes | 250 |
| 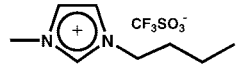 | 1-butyl-3-methylimidazolium trifluoromethanesulfonate | Yes | 250 |
| 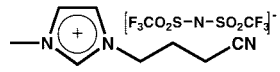 | 1-(3-cyanopropyl)-3-methylimidazolium Bis(trifluoromethanesulfonyl)imide (CN) | Yes | 250 |
| 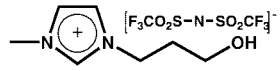 | 1-(3-hydroxypropyl)-methylimidazolium Bis(trifluoromethanesulfonyl)imide (OH) | Yes | 200 |
| 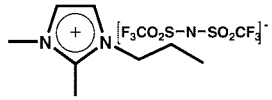 | 1-propyl-2,3-dimethylimidazolium Bis(trifluoromethanesulfonyl)imide | Yes | 250 |
| 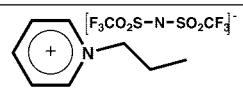 | 1-propylpyridinium- Bis(trifluoromethanesulfonyl)imide | Yes | 250 |
| 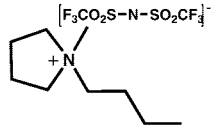 | 1-butyl-1-methylpyrrolidinium Bis(trifluoromethanesulfonyl)imide | No | 250 |
| 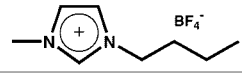 | 1-Butyl-3-methylimidazolium tetrafluoroborate | No | 250 |
| 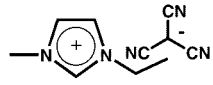 | 1-ethyl-3-methylimidazolium tricyanomethide | No | 250 |

10 h (*C*/10). All $LiFePO_4$ samples were found to be electrochemically active. However, again for brevity, we will solely report data (Figure 9a) for the samples showing the best performances, that is to say, for the samples made in EMI-TFSI and in C10-based EMI-TFSI, which turn out to have particles size of 300 and 500 nm, respectively. For the former, the voltage composition curve shows at a *C*/10 rate a reversible and sustainable capacity of 150 mA h $g^{-1}$, which is somewhat spectacular knowing that this sample was neither chemically coated nor ever treated at temperatures greater than 250 °C but simply ball-milled with 15% SP carbon for 15 min. Besides, the samples show excellent capacity retention (Figure 9 inset), though their rate capabilities are far from today's state of the art electrodes based on carbon nanopainted $LiFePO_4$ powders; the latter are made from traditional pyrolysis at 700 °C of sugar precursors[3,4,10]

## Discussion

We have reported the use of ionic liquids as a safe alternative to organic or aqueous solvents to synthesize inorganic compounds. $LiFePO_4$ was selected because of its worldwide importance as electrode material for concept demonstration, but it should be realized that many other materials can easily be obtained as well using this versatile synthesis approach. Throughout the paper, we capitalized on the richness of the ionic liquid chemistry by acting on the natures of anions ($TFSI^-$, $BF_4^-$, $CF_3SO_3^-$, $C(CN)_3^-$, $Cl^-$) and cations charge center (imidazolium, pyrrolidinium, pyridinium) and increasing chain length (C2−C18) on imidazolium cations so as to change the physicochemical characteristics (polarity, surface tension) of these new classes of solvents. We revealed the feasibility of synthesizing

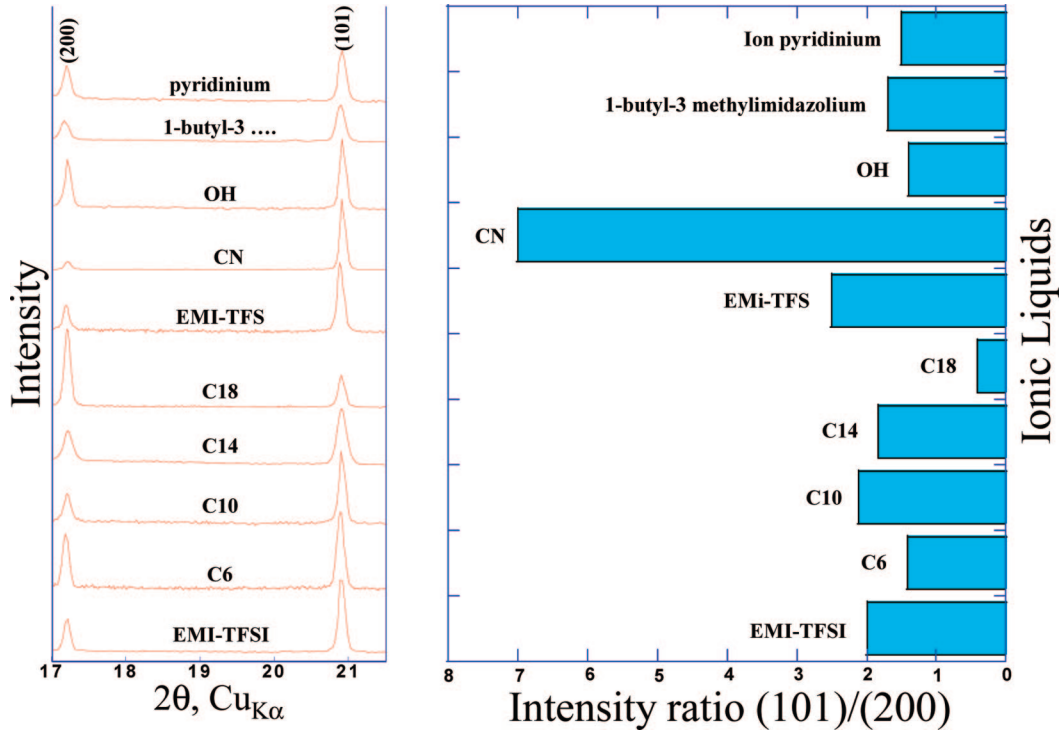


**Figure 5.** Effect of the nature of the ionic liquid on the (101)/(200) XRD intensity ratio. Note that 1-(3-cyanopropyl)-3-methylimidazolium bis(trifluoromethanesulfonyl)imide ionic liquid (CN-based) favors the [010] growth direction, in contrast to the 1-octadecyl-3-methylimidazolium is(trifluoromethanesulfonyl)imide ionic liquid (C18), which favors particle growth perpendicular in the [200] direction.

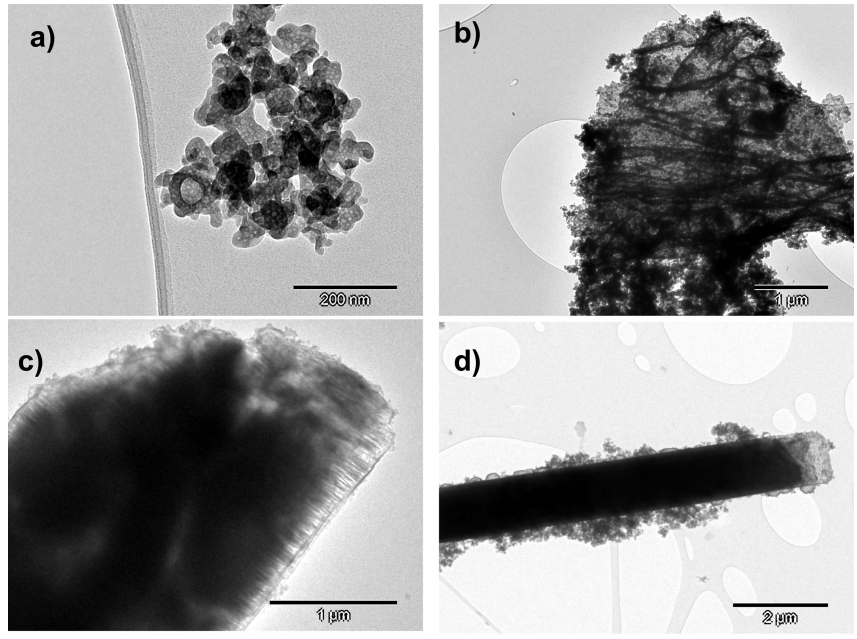


**Figure 6.** TEM bright-field images realized on a $LiFePO_4$ sample grown in a CN-based ionic liquid. The different steps leading to the formation of large $LiFePO_4$ single crystal formation are shown within (a) the nucleation of nanometric LFP particles (100 nm); (b) the growth of small needles of LFP; and (c, d) the pile up of these small needles to form large needles (larger than 1 $\mu$m × 10 $\mu$m).

$LiFePO_4$ in most of the ILs we tried except for 1-butyl-1 methylpyrrolidinium bis(trifluoromethanesulfonyl)imide (BMPy-TFSI), 1-butyl-3-methylimidazolium tetrafluoroborate and 1-ethyl-3 methyl imidazolium chloride (EMI-Cl) pointing to the polarity of either the cation itself ($BMPy^+$ $\mu \approx 0$ D), or to the tight pair of ions (EMI-Cl). Besides, we showed that $LiFePO_4$ powders can be grown either needle-like along the [010] direction by acting on the $EMI^+$ cation chemistry via the attachment of CN rather than OH ending groups, which modifies the polar character of the reacting media and consequently its solvating properties, or platelet-like along the [200] direction by decreasing the polarity via the use of a C18-based ionic liquid. Besides, it should be noted that CN groups are known to have a strong solvating character for $Fe^{II}$-species as from the stability of cyanocomplexes ($Fe(CN)_6^{4-}$).

Trying to reconcile all of the above findings, we reached the fundamental question regarding the role and impact of

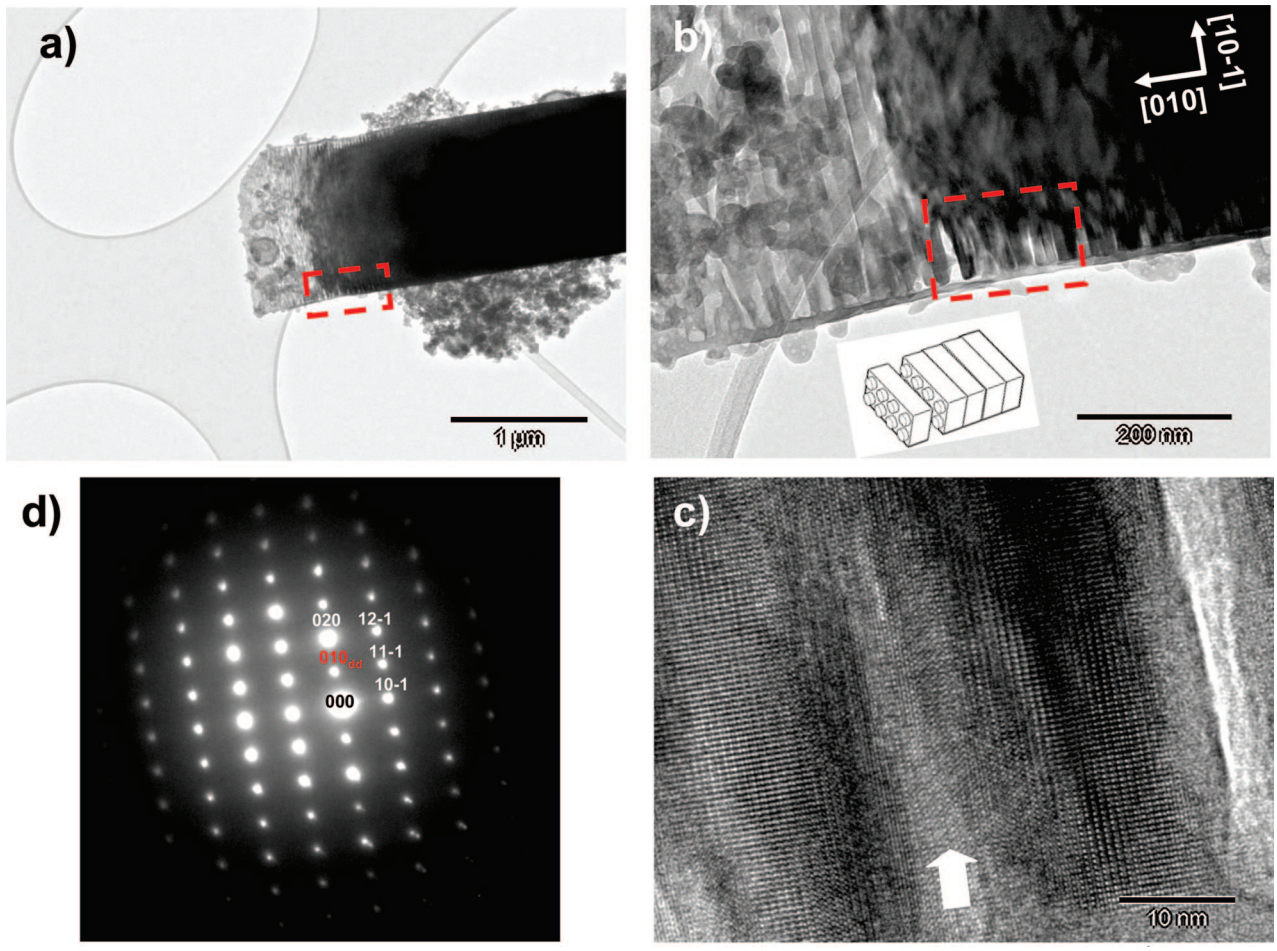


**Figure 7.** TEM images of a $LiFePO_4$ sample grown in a CN-based ionic liquid and showing the quality of the stacking of the small needles forming a large one (a) from an enlarged view taken on the edge of the large needle; (b) the piling up of the small needles could be observed and compared to the assembling of Lego blocks (in inset). The quality of the assembling is confirmed by both (c) the SAED pattern showing well-defined spots and preferential orientation and (d) the HRTEM image showing the perfect alignment of atoms. The white arrow shows the "cementing" zone.

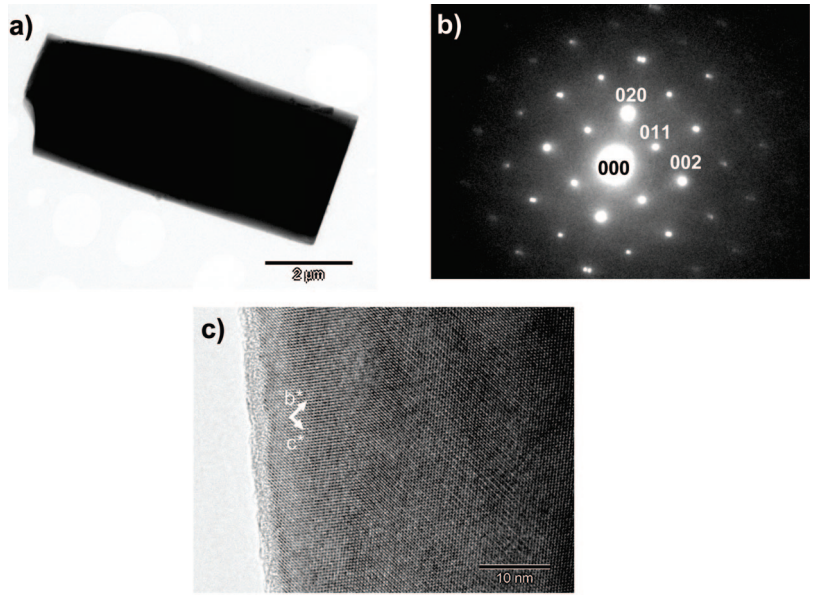


**Figure 8.** TEM study realized on a $LiFePO_4$ sample, grown in a C18-based ionic liquid and showing (a) a bright-field image of the particles (6 $\mu$m × 4 $\mu$m), (b) the corresponding SAED pattern that could be indexed and is in agreement with the preferential orientation observed by XRD, and (c) the HRTEM image of the edge of the particle.

the ionic liquid on $LiFePO_4$ nucleation/growth, and how the ionic liquid can act as a structural directing agent. HRTEM studies indicate that the $LiFePO_4$ growth does occur from the solution, which implies some partial solubility of the precursors although we pertinently know that, whichever precursors used, they have a limited degree of solubility, at

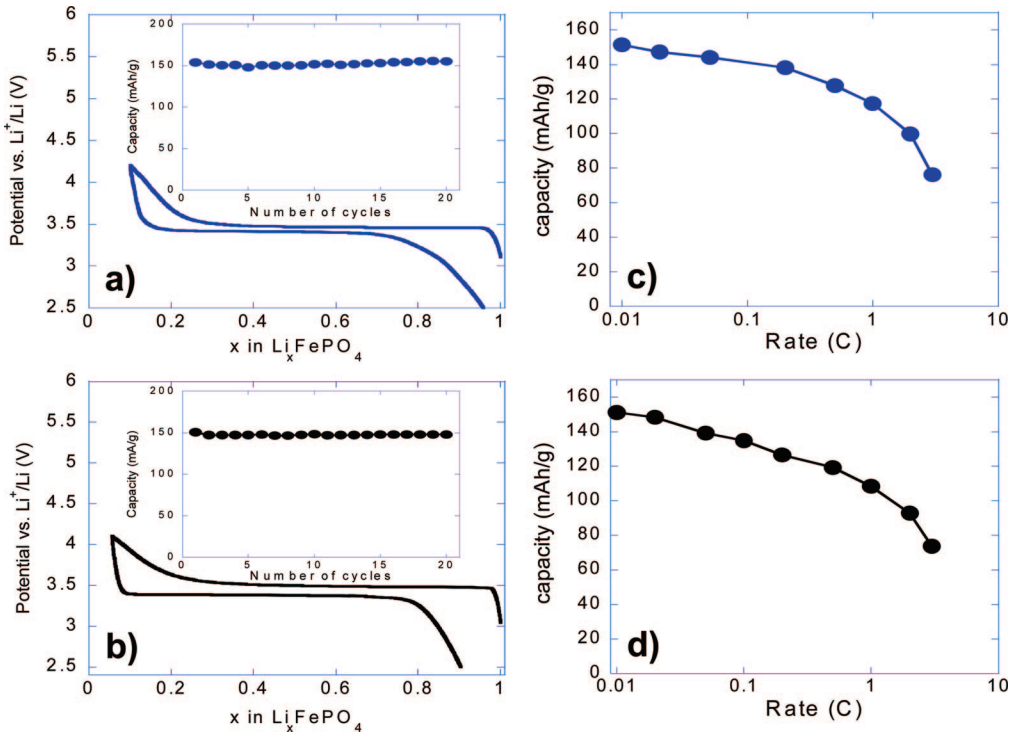


**Figure 9.** Room-temperature voltage-composition curves together with the capacity retention (inset) are reported in (a) and (b) for samples made of an EMI-TFSI and C10-based ionic liquid media, respectively. The positive electrodes, containing 7−10 mg of active material per $cm^2$, were made by ball milling (Spex 800 for 15 min) $LiFePO_4$ powders and carbon SP (carbon black from MM, Belgium) mixtures in 85−15% weight ratio. The power rate capabilities of such electrodes, determined using a "signature curve" are shown in (c) and (d).

least prior to the precursor decomposition. Therefore, the ionic liquid facilitates transport, bringing the reacting species together. Additionally, DSC results have clearly shown that $LiFePO_4$ growth does not occur until the precursors begin to decompose into soluble reacting species, which react to first form nanoparticles of $LiFePO_4$ as observed by HRTEM. Now let us turn to the step-by-step growth process by first having the nanoparticles piling into needles growing along the $[10\bar{1}]$ direction prior to stacking together to favor single crystal growth in the [010] direction (Figures 6 and 7). To get an insight into this growth mechanism, we must go back to the energetic aspect of a particle formation, a process ruled by the need to minimize the overall change in free energy ($\Delta G$), which is the sum of the change in free energy of condensation ($\Delta G_c$) and the free energy change due to the creation of the solid/liquid interface ($\Delta G_s$). It therefore results from a competition between core ($\Delta G_c < 0$) and surface free energy ($\Delta G_s > 0$). This interface/surface energy $\Delta G_s = \Delta(\text{surface}\cdot\gamma)$, where $\gamma$ enlists surface tension and strain, can occasionally overwhelm the core energy when downsizing the particles, hence enabling the feasibility of reversing polymorphs stabilization (growth of $TiO_2$ anatase over $TiO_2$ rutile at the nanoscale level) for very fine particles.[21] Moreover, the $\gamma$ values are well-known to differ from one crystallographic *hkl* face to another, and this means that, for a given particle, the global surface energy is the sum of the individual contributions of each face ($\Sigma S_{hkl}\cdot\gamma_{hkl}$). This can easily account for the observed microscopic mechanism. Indeed, one can assume the overall free energy value to be minimized by the growth of the LFP particles along the $[10\bar{1}]$ direction until a maximum needle length (and therefore free energy value) is reached. Only a coarsening and growth of these needles along a perpendicular direction (i.e., [010]) can then match the minimum energy criterion.

Within this context, we should simply recall that truncated edge metal oxide surfaces are composed of ions of unsatisfied coordination, which means that some atoms have unsatisfied electric charges thus leading to a surface energy landscape, the relief of which depends on the crystal structure. Such edge-free energies are suggested to play an important part in determining the sequence of shape changes when particles in nonequilibrium shapes are growing. One belief is therefore that the needlelike particle obtained in CN-based EMI ionic liquid can be explained on the basis of competing energy surfaces. The initial growth of the needles results from the oriented aggregation of isotropic nanoparticles occurring on the most energetic surfaces (namely on the tip of the needles). Although the specific surface tension for the lateral needle surface is smaller than the specific surface tension for the needle tip, the total resulting surface lateral energy can occasionally become greater than the needle tip surface energy. When such a threshold is reached, the needle particle can move/rotate in order to get the juxtaposition of the particles so as to minimize interfacial energy. The substantial ionic force of the IL screens the repulsions between the charge surfaces, and makes aggregation easy. It results in the growth of metastable aggregates that will lead to a highly crystalline particle via Ostwald ripening. The latter can occur only via mass transport implying a solution growth mechanism. Because of such a proposed mechanism, it does not come as a surprise that the obtained particles' size and shape

(21) McHale, J. M.; Auroux, A.; Perrotta, A. J.; Navrotsky, A. *Science* **1997**, 277.
(22) Gribb, A. A.; Banfield, J. F. *Am. Mineral.* **1997**, *82*, 717–728.

depend on the nature of the ionic liquid, solvating power, polarity, and aptitude to specifically absorb on one of the surfaces (e.g., to play a structural directing agent role).

Interestingly, we note that a long alkyl chain favors a different growth orientation. Most likely this result is rooted in a lower solvating power and weaker ionic strength of the C18-based ionic liquid as compared to a C6, C10 or C14 one, so that surface energy minimization will take place via a different mechanism. It is reasonable to expect that well-selected ionic liquids could be used as structure-directing agents to prepare tailor-made powders, to stabilize polymorphs, and so on. This issue will most certainly find a rationalized use very quickly, thanks to the importance of this synthetic route and of the materials they give access to, and to the rapidly growing IL scientific community. Finally, this approach, which presents direct advantages over: (1) the molten salts methods that usually require higher temperatures and a specifically selected solvent to dissolve the salt; or (2) the hydrothermal reactions that require the cumbersome use of autoclaves, can be extended to the low-temperature synthesis of numerous already known phases as well as the design and stabilization of new ones[23] opening then a multitude of opportunities to design ionic liquid on demand to target a specific compound or a specific morphology.

CM803259X

(23) Recham, N. Tarascon, J.-M. Armand, M. CNRS Patent application Fr 08/03233.